Characterization of Charge Transfer Processes in Self-Assembled Monolayers by High-Pressure Electrochemical Techniques

María T. Cruañes,[†] Harry G. Drickamer, and Larry R. Faulkner*

Department of Chemistry, University of Illinois, 600 South Mathews, Urbana, Illinois 61801

Here we report the first high-pressure investigation of redox processes in surface-confined monolayers. We have explored the electrochemical behavior of ferrocene-terminated self-assembled monolayers (SAMs) on gold electrodes immersed in aqueous solutions containing 1 M NaClO₄. Electrochemical measurements conducted at hydrostatic pressures ranging from 0.001 to 6 kbar (1 kbar ≈ 1000 atm) show that the electron-transfer reaction for ferrocene in the monolayer is restricted with the application of pressure, whereas the same reaction for ferrocene in solution is not. The dependence of the cyclic voltammetric peak redox potentials on pressure reveals that the oxidation of the ferrocene within the monolayer becomes thermodynamically and kinetically more difficult at high pressures. At pressures above 1—2 kbar, positive volumes of reaction are associated with the oxidation process, indicating that the oxidation step involves an increase in volume. We also found positive volumes of activation for the oxidation process and concluded that the transition step involves a volume expansion that is coupled with the charge transfer step. A structural transformation that allows for ion complexation upon oxidation of surface-confined ferrocene may be responsible for the volume increase. Different monolayer samples, exhibiting different voltammetric responses, appear to impose different volume constraints on the charge transfer reaction and, therefore, present different pressure responses within a general common trend. These results point out the importance of structural and environmental effects, via steric constraints, on electron transfer processes in surface-confined monolayer assemblies.

Introduction

High-pressure techniques have been established as essential in the investigation of a wide range of properties in solids, liquids, and solutions.[1-6] Mainly, these techniques permit the isolation of effects that are purely dependent on the volume.[2] Here we report for the first time the application of pressure to the in-situ characterization of an interfacial molecular assembly and electron transfer processes within it. The combination of electrochemistry and high pressure[24] has allowed us to explore the kinetics and thermodynamics of electroactive monolayers in the light of compression effects. During the last decade a great deal of effort has been devoted to the study of redox active self-assembled monolayers; in particular, those containing ferrocene functionalities have received the most attention.[7-23] As with any high-pressure determination, the unique feature of the work presented here is that it yields information on the volume requirements that might be involved in the electron transfer process. The following thermodynamic expressions relate volume changes (volumes of reaction and volumes of activation) to measurable quantities, such as redox potential and rate constants.

The change in standard redox potential ($E°$) with respect to pressure at constant temperature is

$$(\partial E°/\partial P)_T = (-1/nF)\Delta V° \qquad (1)$$

where $\Delta V°$, the standard volume of reaction, is defined as the difference between the sum of the standard molar volume of the products ($v°_p$) and the sum of the standard molar volume of the reactants ($v°_r$):

$$\Delta V° = \sum v°_p - \sum v°_r \qquad (2)$$

According to (1), a reduction process that involves a net decrease in volume ($\Delta V° < 0$) is favored with compression,

* Author to whom correspondence should be addressed.

†Present address: Higuchi Biosciences Center, University of Kansas, 2095 Constant Ave., Lawrence, KS 66047.

⊗ Abstract published in *Advance ACS Abstracts,* September 1, 1995.

(1) Drickamer, H. G. *Annu. Rev. Mater. Sci.* **1990,** *20,* 1—17.
(2) Weber, G.; Drickamer, H. G. Q. *Rev. Biophys.* **1983,** *16,* 1.
(3) Hills G. J. *Symp. Soc. Exp. Biol.,* **1972,** *26,* 1—26.
(4) Hamann, S. D. *Physico-Chemical Effects of Pressure;* Butterworths: London, 1957.
(5) Bridgman, P. W. *The Physics of High Pressure;* G. Bell & Sons, London: 1949.
(6) Liu, G.; Mackowiack, M.; Li, Y; Jonas, J. *Chem. Phys.* **1990,** *149,* 165.
(7) Porter, M. D.; Bright, T. B.; Allara, D. L.; Chidsey, C. E. D. *J. Am. Chem. Soc.* **1987,** *109,* 3559.
(8) Hickman, J. J.; Zou, C.; Ofer, D.; Harvey P. D.; Wrighton, M. S.; Laibinis, P. E.; Bain, C. D., Whitesides, G. M. *J. Am. Chem. Soc.* **1989,** *111,* 7271.
(9) Chidsey, C. E. D.; Bertozzi, C. R.; Putvinski, T. M., Mujsce, A. M. *J. Am. Chem. Soc.* **1990,** *112,* 4301.
(10) Chidsey, C. E. D.; Loiacono, D. N. *Langmuir* **1990,** *6,* 682.
(11) Chidsey, C. E. D. *Science* **1991,** *251,* 919.
(12) Hickman, J. J.; Ofer, D.; Laibinis, P. E.; Whitesides, G. M.; Wrighton, M. S. *Science* **1991,** *252,* 688.
(13) Hickman, J. J.; Ofer, D.; Zou, C.; Wrighton, M. S.; Laibinis, P. E.; Whitesides, G. M. *J. Am. Chem. Soc.* **1991,** *113,* 1128.
(14) Collard, D. V.; Fox, M. A. *Langmuir* **1991,** *7,* 1192.
(15) Uosaki, K.; Sato, Y.; Kita, H. *Langmuir* **1991,** *7,* 1510.
(16) (a) Rowe, G. K.; Creager, S. E. *Langmuir* **1991,** *7,* 10, 2307; (b) Creager, S. E.; Rowe, G. K. *Anal. Chim. Acta* **1991,** *246,* 233.
(17) Hong, H; Mallouk, T. E. *Langmuir* **1991,** *7,* 2362.
(18) Everett, R. W.; Welch, T. L.; Reed, L.; Fritsch-Faules, I. *Anal. Chem.* **1995,** *672,* 292.
(19) Walczak, M. M.; Popenoe, D. D.; Deinhammer, R. S.; Lamp, B. D.; Chung, C.; Porter, M. D. *Langmuir* **1991,** *7,* 2687.

(20) Popenoe, D. D.; Deinhammer, R. S.; Porter, M. D. *Langmuir* **1992,** *8,* 2521.
(21) Tsutsumi, H.; Furumoto, S.; Morita, M.; Matsuda, Y. *J. Electrochem. Soc.* **1992,** *139,* 6, 1522.
(22) Clark, B. J.; Cleland, W. E.; Hussey, C. L. *J. Electrochem. Soc.* **1992,** *139,* 11, L107.
(23) (a) Curtin, L. S.; Peck, S. R.; Tender, L. M.; Murray, R. W; Rowe, G. K; Creager, S. E. *Anal. Chem.* **1993,** *65,* 386. (b) Peck, S. R.; Curtin, L. S.; Tender, L. M.; Carter, M; Terrill, R. H.; Murray, R. W; Collman, J. P.; Little, W. A.; Duan, H. M.; Hermann, A. M. *J. Am. Chem. Soc.* **1995,** *117,* 1121.
(24) Cruañes, M. T.; Drickamer, H. G.; Faulkner, L. R., *J. Phys. Chem.* **1992,** *96,* 24, 9888—92.

while one that involves a net increase in volume ($\Delta V° > 0$) is disfavored with compression.

The same principle can be extended to the rates of reactions. The change in volume that occurs when the activated state is formed from the reactants is called volume of activation ($\Delta V^{\ddagger}$). In terms of the transition state theory, the rate of reaction is

$$k = A \exp(-\Delta G^{\ddagger}/RT) \quad (3)$$

where A is the pre-exponential factor and $\Delta G^{\ddagger}$ is the free energy of activation. Then, assuming A to be pressure independent,

$$\partial(\ln k)/\partial P = -1/RT\Delta V^{\ddagger} = -1/RT(v^{\ddagger} - \sum v_{\text{r}}) \quad (4)$$

It follows that if the activated complex has a smaller partial molar volume than the reactants ($\Delta V^{\ddagger} < 0$), the reaction is accelerated by the application of pressure, whereas it is retarded if the partial molar volume of the activation complex is larger than that of the reactants ($\Delta V^{\ddagger} > 0$).

We have prepared self-assembled monolayers (SAMs) of ferrocene-terminated 1-undodecanethiol on polycrystalline gold electrodes in contact with $NaClO_4$ aqueous solutions, and we have explored their electrochemical behavior at pressures that range from 0.001 to 6 kbar (1 kbar $\approx$ 1000 atm). We found that the redox potential shifts positively at pressures above 1–2 kbar, and that the rate of oxidation decreases under compression. Consequently, positive volumes of reaction and activation are associated with the oxidation process, indicating that a volume expansion accompanies the electron transfer step. Our measurements reveal that the volume requirements of the electron transfer process can vary from sample to sample and strongly suggest that these requirements are related to the spatial characteristics of each sample. These results point out the importance of structural and environmental effects, via steric constraints, on electron transfer processes in surface-confined monolayer assemblies.

Materials and Methods

The high-pressure setup used for the experiments is reported elsewhere,[24] except that planar disk gold electrodes (2 mm diameter) were used instead of cylindrical ones. Prior to modification, the gold electrodes were polished with Buehler diamond paste (1 μm), sonicated in Millipore water, polished with diamond paste (0.25 μm), and, finally, sonicated again in Millipore water. Usually, after polishing, a cyclic voltammetric scan was run in 0.1 M H_2SO_4 between −200 and 1600 mV vs Ag/AgCl, NaCl (3 M) (BAS), and the results were compared to those typically obtained for a clean gold electrode. If necessary, the electrodes were electrochemically cleaned in 0.1 M H_2SO_4 by stepping the electrode potential between −200 and 1600 mV vs Ag/AgCl, NaCl (3 M) (BAS). After polishing and cleaning, the electrodes were dipped in a 1 mM ethanolic solution of ferroceneundodecanethiol, while the solution was purged with in-house nitrogen during the first 5 min. Then the cell was sealed, and modification took place for the next 24 h. The modified electrodes were removed from the mercaptan solution and then rinsed with ethanol, hexane, ethanol, and finally Millipore water. They were immediately dipped and stored in an aqueous solution of supporting electrolyte, either 1 M $NaClO_4$ or 1 M $NaNO_3$, for at least 24 h. After this equilibration period, the electrochemical responses of these monolayers were found to be very stable over a period of weeks. The SAM-modified electrodes were transferred to the high-pressure cell and apparatus a few hours before the pressure experiment. The working electrode compartment of the cell contained the same supporting electrolyte in which the modified working electrode had been equilibrated. The reference
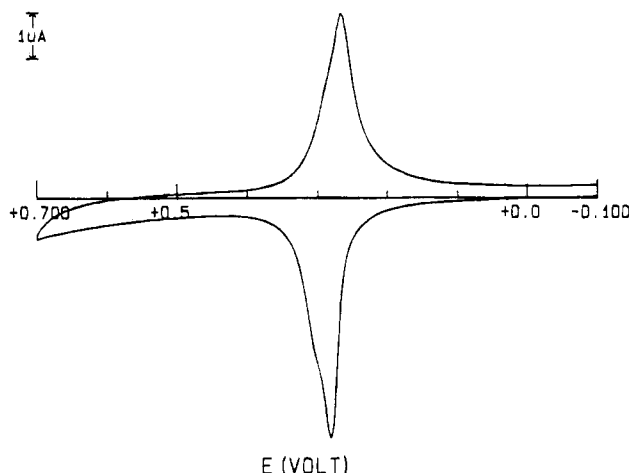

Figure 1. Ambient-pressure cyclic voltammogram of ferrocene-terminated undodecanethiol SAM on a gold electrode immersed in aqueous 1 M $NaClO_4$ (sample 3): Scan rate, 100 mV/s, vertical scale, 1 μA. Surface coverage $\Gamma = 3.5 \times 10^{-10}$ mol/cm^2.

electrode compartment of the high-pressure cell contained 0.1 M NaCl plus either 1 M $NaClO_4$ or 1 M $NaNO_3$ to match the supporting electrolyte in the working electrode compartment.

The roughness of the bare gold electrodes was determined by measuring the charge that evolved during reduction of the superficial oxide formed during a positive potential sweep in 0.1 M H_2SO_4 acid. The area under the reduction wave is proportional to the amount of gold oxide which, in turn, can be converted to real area by using the appropriate coefficient,[25] 0.43 mC/cm^2. The ratio of real to geometrical surface area is called the roughness factor. The roughness factor of our electrodes varied between 2.1 and 3.0 with an average value of 2.5. Undodecanethiolferrocene was synthesized by Dr. Chaofeng Zou according to procedures outlined elsewhere.[12,26] Ferrocene methanol (Aldrich) was used as received.

Cyclic voltammetric (CV), chronocoulometric (CC), and chronoamperometric (CA) experiments were done using a BAS 100A or 100B Potentiostat. Impedance measurements were performed on an EG&G Princeton Applied Research (PAR, Princeton, NJ) Model 378 Impedance System.

Unless otherwise indicated, potential values are measured against the high-pressure reference electrode [Ag/AgCl, NaCl (0.1 M)] described elsewhere;[24] therefore, pressure-induced redox potential changes include changes corresponding to those of the Ag/AgCl, NaCl (0.1 M) equilibrium. Formal redox potentials ($E°'$s) are calculated from the average of anodic and cathodic peaks of cyclic voltammograms. At high pressures, where the kinetics of the redox reaction show a degree of asymmetry, owing to the anodic and cathodic peak potentials not being equally affected by compression, we denote the average of the peak potentials as E instead of the thermodynamic $E°'$. Surface coverage values were calculated by integration (BAS 100B potentiostat software) of the area under the anodic CV wave. All experiments were conducted at ambient temperature.

Results and Discussion

Ambient Pressure Results. Figure 1 shows a cyclic voltammogram for a ferroceneundodecanethiol monolayer on a polycrystalline gold electrode dipped in aqueous 1 M $NaClO_4$. The voltammetric response exhibits thin-layer behavior, indicative of surface-confined species, with peak currents proportional to the scan rate at least up to 10 V/s. Although voltammetric waves for all samples that we have prepared show typical thin-layer behavior, with peak currents proportional to scan rates and peak separations that range from 5 to 30 mV at a sweep rate

(25) Gileadi, E.; Kirowa-Eisner, E.; Penciner, J. *Interfacial Electrochemistry—An Experimental Approach*; Addison-Wesley Publishing Co., Inc.: Reading, MA, Massachussets, 1975.

(26) Zou, C.; Wrighton, M. S. *J. Am. Chem. Soc.* **1990**, *112*, 7578–84.

of 10 mV/s, not all of them present the exact same appearance. Some showed peaks with shoulders, or even extra peaks, which are evidence of heterogeneities or different domains in the monolayer. These observations are in agreement with those reported previously for pure or concentrated ferrocene-terminated alkanethiol monolayers.[14-16] We found no clear correlation between the observed shape of the cyclic voltammetric waves and the sample preparation procedure, except that longer equilibration times in electrolyte tended to give rise to single waves rather than multiple waves. (In our case, we also attribute the heterogeneities in the responses to the roughness of the electrodes employed. The electrodes available for high-pressure measurements were solid polycrystalline gold electrodes with a degree of roughness larger than is typical of gold-evaporated films.) The results presented and discussed here correspond to samples exhibiting single anodic and cathodic CV waves without pronounced shoulders. The formal redox potential corresponding to the surface ferrocene couple in 1 M NaClO$_4$ is $E^{\circ\prime}_{SAM} \approx 360$ mV vs Ag/AgCl, NaCl (3 M), which is more positive than $E^{\circ\prime}$ for the dissolved couple in the same aqueous electrolyte, i.e., $E^{\circ\prime}_{Sol} \approx 200$ mV vs Ag/AgCl, NaCl (3 M). The more positive formal potential indicates that the reduction process becomes energetically more favorable upon surface immobilization of the ferrocene couple. This phenomenon may be explained by the lower dielectric medium[20] *and* steric constraints encountered by the ferrocene in the surface assembly. The alkane-like *and* crowded environment of the assembly may destabilize the charged ferrocenium in favor of the neutral ferrocene. As we discuss below, $E^{\circ\prime}_{SAM}$ becomes more negative as the concentration of NaClO$_4$ increases while $E^{\circ\prime}_{Sol}$ remains nearly constant. This counterion concentration dependence reveals that ion-pairing between perchlorate ion and ferrocenium eases the oxidation of ferrocene in the monolayer.

We found that our cyclic voltammograms exhibit narrow peaks with FWHM (full width at half maximum) that are smaller than the ideal value of 90.6 mV expected for a monolayer of noninteractive sites. The observed widths ranged from 20 to 70 mV, indicating that strong attractive interactions between redox centers exist in these monolayers.[27] Due to the low affinity of the ferrocene for the aqueous medium, we envision the alkyl chains folded, rather than extended toward the aqueous solvent. In this way the ferrocene groups would be buried within the monolayer in a less polar environment or bent to bring the head groups together, creating aggregates of ferrocene within the microstructure. This model is consistent with the submonolayer coverage values that we measure for our samples (typically N = 2 × 10^{-11} mol). Taking into account the roughness of the electrodes, ferrocene surface concentrations range between one-half and two-thirds of a full monolayer, with an average of $\Gamma = 2.8 \times 10^{-10}$ mol/cm^2. (Complete coverage, based on the projected area of the ferrocene group,[9] is 4.5×10^{-10} mol/cm^2).

The importance of counterion availability in the charge-transfer thermodynamics of the ferrocene-containing assemblies is evident from the dependence of the formal potential of the surface-confined couple on anion concentration and identity. Table 1 shows that the oxidation of ferrocene in the monolayer is thermodynamically easier in the presence of the more lipophilic ions[16a] (perchlorate and tosylate), suggesting that it forms the strongest ion complex with them. In agreement with other reports,[15,16a]

(27) Laviron, E. *J. Electroanal. Chem.* **1972**, *39*, 1; **1974**, *52*, 395; **1979**, *100*, 263; **1979**, *105*, 25; **1979**, *105*, 35.

**Table 1. Redox Potential for FeCp$_2$$^+$/FeCp$_2$ in SAM^a**

supporting electrolyte anion (1 M)	$E^{\circ\prime}$ (mV)^b	supporting electrolyte anion (1 M)	$E^{\circ\prime}$ (mV)^b
perchlorate	360	chloride	485
tosylate	420	biphosphate	500
nitrate	450		

^{a} $E^{\circ\prime}$ for dissolved OHCH$_2$ FeCp$_2$$^+$/FeCp$_2$ in 1 M NaClO$_4$ is ≈200 mV. ^{b} $E^{\circ\prime}$ vs Ag/AgCl/NaCl (3 M); scan rate = 100 mV/s.

we have also found that the formal redox potential ($E^{\circ\prime}$) of ferrocene in the monolayer decreases as the concentration of perchlorate or nitrate ions increases, clearly indicating the formation of ion pairs in the assembly. This dependence is not observed (ref 16, this work) for dissolved ferrocene ethanol or ferrocenemethanol, for which $E^{\circ\prime}$ is ≈200 mV vs Ag/AgCl, NaCl (3 M) in aqueous solutions containing either NaClO$_4$ or NaNO$_3$, 1 M or 0.1 M. This contrasting behavior can be explained by the need to neutralize the excess charge that builds up at the interface upon oxidation and to stabilize the ferrocenium ion in the nonpolar and crowded environment of the assembly.

High Pressure Results. *Cyclic Voltammetric Studies.* It is revealing to look at the effect of high pressures on the electrochemical behavior of these alkylferrocene assemblies. In Figure 2 we present two series of CV's depicting the pressure-induced changes. Upon compression, peak separation increases, waves broaden and become less symmetric, surface coverage seems to decrease, and the typical thin-layer response disappears, as if electroactive material was not bound to the electrode surface any longer and had to diffuse from solution. Above 5−6 kbar, no significant electrochemical response is observed. It is remarkable that immediately after pressure reversal the initial ambient-pressure response is always recovered. This behavior implies that the pressure-induced changes are reversible and that no significant amount of material is lost under pressurization. If electroactive material were lost at high pressure, it is highly unlikely that it would reassemble so quickly on decompression to replicate the original cyclic voltammetric response. Therefore, we conclude that the decrease in surface coverage is only apparent and that the diffusion-like voltammograms encountered at high pressures reflect a decrease in the electron transfer rate constant. We also observe that the anodic peak shifts, broadens, and diminishes in height more than the cathodic one does.

Another feature of the pressure experiment is that the potential (E) of the surface-confined ferrocene/ferrocenium couple shifts in the positive direction at pressures above 1−2 kbar. A plot of E (calculated from the average of anodic and cathodic peaks) vs pressure for one electrode sample can be found in Figure 3. This trend, observed for all of our samples, indicates that the reduction process is energetically favored with compression at pressures beyond 1−2 kbar. According to (1), the volume change ($\Delta V = \Delta V^{red}_{SAM}$) involved in equilibrium (5) is negative. Conversely, the oxidation process, which is disfavored by compression, involves a positive volume change (ΔV^{ox}_{SAM}).

$$FeCp_2{}^+ClO_4{}^-(SAM) + Ag(s) + Cl^-(aq) \leftrightarrow$$
$$FeCp_2(SAM) + ClO_4{}^-(aq) + AgCl(s) \quad (5)$$
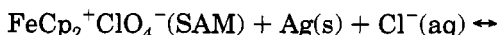
$$\Delta V^{red}{}_{SAM} = v_{FeCp_2(SAM)} + v_{ClO_4{}^-(aq)} +$$
$$v^{\circ}{}_{AgCl(s)} - v_{FeCp_2{}^+ClO_4{}^-(SAM)} - v^{\circ}{}_{Ag(s)} - v_{Cl^-(aq)} < 0$$

where v stands for partial molar volume of the species

(a)

(b)
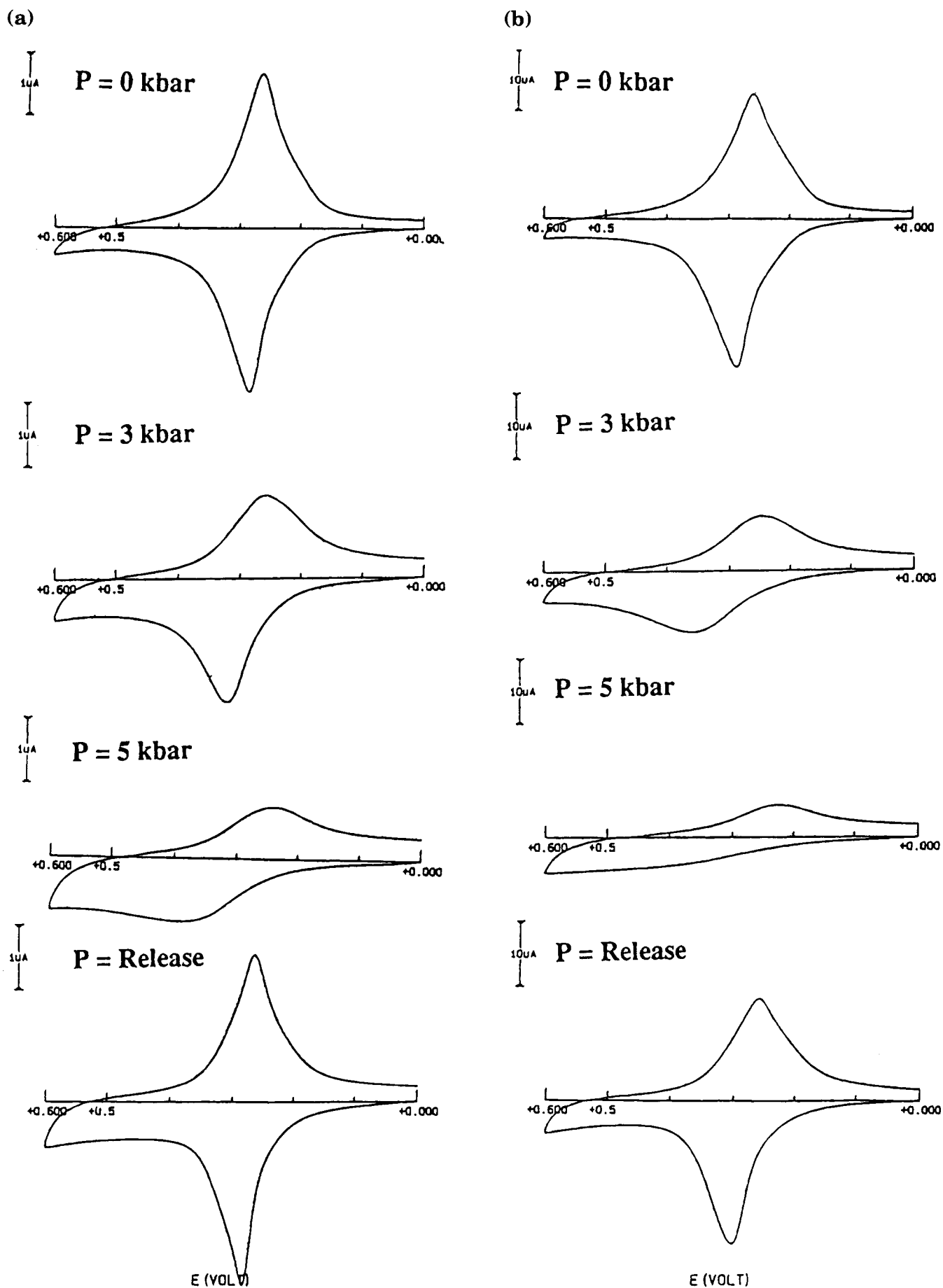
Figure 2. Cyclic voltammograms of ferrocene-terminated undodecanethiol SAM on a gold electrode immersed in 1 M NaClO$_4$ (sample 2) at various pressures: scan rate, (a) 100 mV/s, (b) 1000 mV/s; vertical scale, (a) 1 μA, (b) 10 μA. Ambient-pressure surface coverage Γ = 2.4 × 10^{-10} mol/cm^2.
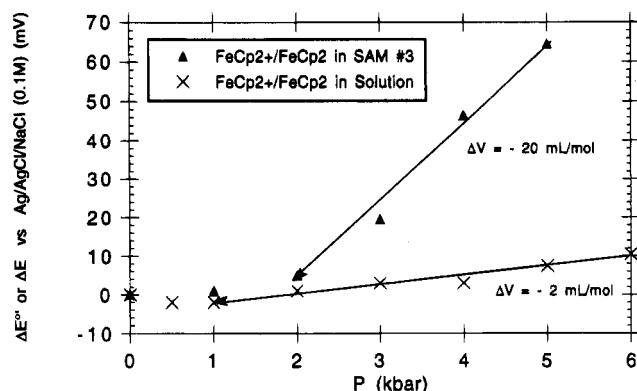
Figure 3. Change in redox potential of ferrocene/ferrocenium couple in SAM immersed in 1 M NaClO$_4$ as a function of pressure (Sample 3, ambient-pressure surface coverage $\Gamma = 3.5 \times 10^{-10}$ mol/cm^2). E is the average of anodic and cathodic peaks of cyclic voltammograms taken at a scan rate of 100 mV/s (ΔE equals E at pressure P minus $E^{\circ\prime}$ at ambient pressure). Change in $E^{\circ\prime}$ for α-ferrocenemethanol/ferrocenium (water soluble ferrocene analog), dissolved in the same electrolyte, is shown for comparison ($\Delta E^{\circ\prime}$ equals $E^{\circ\prime}$ at pressure P minus $E^{\circ\prime}$ at ambient pressure). Volumes of reaction for the reduction process extracted from the linear slope are $\Delta V^{red}_{SAM} = -20$ mL/mol ($P > 2$ kbar) and $\Delta V^{red}_{Sol} = -2$ mL/mol ($P > 1$ kbar).

indicated by the subscript. For comparison, we also show in Figure 3 the pressure dependence of $E^{\circ\prime}$ for the water soluble ferrocene/ferrocenium couple in aqueous 1 M NaClO$_4$ [equilibrium (6)].

$$FeCp_2^+(aq) + Ag(s) + Cl^-(aq) \leftrightarrow$$
$$FeCp_2(aq) + AgCl(s) \quad (6)$$
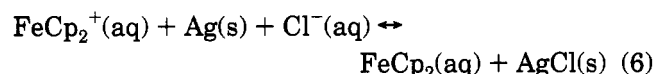
$$\Delta V^{red}_{Sol} = v_{FeCp_2(aq)} + v^{\circ}_{AgCl(s)} - v_{FeCp_2^+(aq)} -$$
$$v^{\circ}_{Ag(s)} - v_{Cl^-(aq)} < 0$$

In the same pressure range, the reduction of dissolved ferrocenium seems to be slightly favored with compression also. However, the effect of pressure is remarkably more pronounced for the surface-confined ferrocene/ferrocenium couple. In fact, ΔV_{SAM} and ΔV_{Sol} differ by an order of magnitude. Since the volume change for the reference electrode half-reaction is the same for both (5) and (6), we have that

$$v_{FeCp_2(SAM)} + v_{ClO_4^-(aq)} - v_{FeCp_2^+ClO_4^-(SAM)} <$$
$$v_{FeCp_2(aq)} - v_{FeCp_2^+(aq)}$$

On the basis of molecular size and solvation, inferred from these, previous results[24] and the "ferrocene assumption",[28] we take $v_{FeCp_2(aq)} \approx v_{FeCp_2^+(aq)}$.
Then,

$$v_{FeCp_2(SAM)} + v_{ClO_4^-(aq)} < v_{FeCp_2^+ClO_4^-(SAM)} \quad (7)$$

Expression (7) indicates that the oxidation of ferrocene in the monolayer involves a volume expansion. This volume expansion experienced by the superficial assembly renders oxidation more difficult under pressure by imposing volume limitations that are absent in solution. Because of the "ferrocene assumption" explained below, we discard *intrinsic* hydration effects as the origin of the volume changes. We propose that the more stringent

Table 2. Volume Change upon Oxidation for FeCp$_2$/FeCp$_2^+$ in SAM (1M NaClO$_4$)

sample	ΔV^{ox}_{SAM} (mL/mol)	sample	ΔV^{ox}_{SAM} (mL/mol)
1	10[a]	4	22[b]
2	10[b]	5[d]	15[c]
3	20[b]		

[a] At $P \geq 2$ kbar. [b] At $P \geq 3$ kbar. [c] At $P \geq 1$ kbar. [d] Supporting electrolyte is 1 M NaNO$_3$ instead of NaClO$_4$.

volume requirements stem from surface confinement of the ferrocene couple. The generation of charge out of the neutral surface assembly could cause or require a structural rearrangement in the monolayer so as to minimize electrostatic repulsion and allow for the incorporation of counterions to neutralize excess positive charge on the ferrocenium. Counterion incorporation is probably made increasingly more difficult as rising pressures may enhance aggregation and disrupt ion-pairing.

Here we would like to explain that the "ferrocene assumption" that we invoke and support with previous data[24] tells us that there is no *intrinsic* preferential hydration of one oxidation form of the couple over the other. (Preferential interactions with neighboring molecules and counterions may still arise from surface confinement as shown here.) For most other non-ion-paired redox compounds dissolved in aqueous solution,[3,4,24,30] the higher charged oxidation state is favored with pressure because of the volume contraction (electrostriction effect[30]) that stems from enhanced hydration around the extra charge. In contrast, the ferrocenium ion is not expected to be significantly more, or less, hydrated than the ferrocene molecule. Therefore, the volume changes observed for ferrocene in the monolayer are unlikely to arise from changes in the hydration shell of the ferrocene/ferrocenium couple upon redox reaction. Also, the existence of ion pairing itself indicates that the ferrocenium ion is not solvated in the monolayer.

Volumes of reaction (ΔV^{ox}_{SAM}'s) for the oxidation process [reverse of equilibrium (5)], for five different samples in either NaClO$_4$ or NaNO$_3$, are shown in Table 2. These ΔV's are calculated by doing least-squares regression of the linear portion of the E vs P curve. At pressures below the linear region, ΔV's are negative or close to zero and in general agreement with the negligible volume changes observed[24] for a couple, such as dissolved ferrocene/ferrocenium, that interacts weakly with the solvent.[24,28] In each monolayer sample, grain boundaries, defect sites, and loose packing[9,14] could create disordered structures in which not all ferrocene groups are equally aggregated or solvent-exposed. The nonuniform ferrocene populations would experience differing volume constraints upon oxidation—reduction. Therefore, we infer that ΔV's are composed of more than one term, i.e., $\Delta V_{SAM} = \sum f_i \Delta V_i$, where f_i is the fraction of one type of redox population, each type corresponding to different local environments and spatial configurations. Heterogeneities within each sample must translate into heterogeneities among the various samples and give rise to differing ΔV's for different samples (note that the volume change for the reference electrode half-reaction[24] is the same for all samples).

Table 3 shows that peak separations for surface-confined ferrocene increase as a function of pressure, indicating that the kinetics of electron transfer become more sluggish under compression (peak separations are not substantially affected by pressure for ferrocene dissolved in aqueous solution). Also, unlike the pressure-induced potential changes observed for ferrocene in solution, the potential

(28) Popovich, O. In *Treatise on Analytical Chemistry*, 2nd ed.; Kolthoff, I. M., Elwing, P. J., Eds.; Wiley: New York, 1978; Part I, Vol. I, p 711.
(29) Padova, J. *J. Chem. Phys.* **1963**, *39*, 1552.

(30) Hamann, S. D., *Rev Phys. Chem. Jpn.* **1980**, *50*, 147.

Table 3. CV Peak Separation vs Pressure $FeCp_2/FeCp_2^+$ in SAM (100 mV/s)

P (kbar)	ΔE_p (mV)		P (kbar)	ΔE_p (mV)	
	sample 3^a	sample 5^b		sample 3^a	sample 5^b
0	24	19	3	85	58
1	34	23	4	153	90
2	48	38	5	217	147

^{a} In $NaClO_4$ (1 M). ^{b} In $NaNO_3$ (1 M).
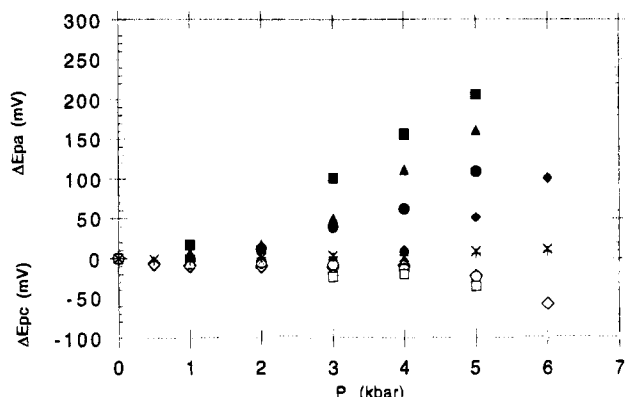
Figure 4. Pressure-induced potential shifts for the cyclic voltammetric oxidation (ΔE_{pa}) and reduction (ΔE_{pc}) peaks of the ferrocene/ferrocenium couple in several different SAM samples dipped in aqueous 1 M $NaClO_4$ are compared to those for the same couple dissolved in aqueous 1 M $NaClO_4$. The scan rate was 100 mV/s for all. Key: diamonds, SAM 1; circles, SAM 2; triangles, SAM 3; squares, SAM 4. (Solid symbols are for anodic peaks; hollow symbols are for cathodic peaks). For dissolved ferrocene/ferrocenium: x, anodic peak; +, cathodic peak.

shift observed for ferrocene in the monolayers is not strictly thermodynamic. That is, in contrast with ferrocene in solution, the cathodic (reduction) and anodic (oxidation) peaks do not shift together with pressure. For all of our samples the dependence of anodic peak potential on pressure is more pronounced than that of the cathodic peak (Figure 4). These data provide evidence that greater volume changes (volumes of activation) are involved in the oxidation step. This asymmetry is not surprising considering that volume profiles,[31] unlike energy profiles, can be continuously ascending or descending and do not necessarily show an extremum, so that volumes of activation ($\Delta V^{\ddagger}$) can be either positive or negative (or null). Therefore, it is possible for the forward and reverse steps to be affected differently by pressure, just as it is possible for these steps to be affected differently by temperature. (With temperature the difference is only in the magnitude of the effect, but with pressure the difference is often also in the sign of the effect.) In our case, the asymmetry suggests that the volume expansion associated with the oxidation process would lead to positive volumes of both reaction and activation. We can at least qualitatively say that $\Delta V^{\ddagger}_{ox} > \Delta V^{\ddagger}_{red}$ and that the activation state on oxidation (forward step) is more "product-like" (more like ion-complexed ferrocenium), and on reduction (reverse step) the activation state is less "product-like" (less like uncomplexed ferrocene). Here we would like to add that a "square scheme" in which the reduction step does not follow the exact reverse path of the oxidation is also compatible with the asymmetry depicted in Figure 4. Such a scheme could result from a structural transformation brought upon by redox reaction in the monolayer.

In Figure 4, we also observe that the pressure-induced shifts in peak potential differ from sample to sample. As

explained above, we think that subtle structural variations exist from sample to sample. These variations would cause different spatial arrangements and, therefore, different environments around the ferrocene groups, which in turn would impose different volume requirements on the kinetics of the redox reaction.

Summarizing, we have evidence that the oxidation process is restricted by compression to a larger degree than the reduction is and that a volume increase has to precede, accompany, or follow the oxidation. We reason that the oxidation of neutral ferrocene to charged ferrocenium would perturb the aggregation of the molecules in the monolayer and might then cause or require stretching of an alkyl chain, so as to bring the ferrocenium ion closer to a counterion, and/or inclusion of a desolvated anion to mitigate the electrostatic repulsions. This series of events could give rise to a redox-dependent structural transformation of the monolayer. The steps above, including the desolvation of the perchlorate anion, would involve a volume expansion and would be consistent with the positive volumes of reaction that we found. As we already stated, the volume increase is not due to the reference electrode. Neither can it be totally ascribed to the desolvation of the perchlorate ion; with reported values,[29] we calculate the volume of desolvation of the perchlorate ion to be only 1.6 mL/mol.

Pressures higher than 0.5–1 kbar appear to be required to cause the most noticeable effects on the charge transfer reactions in the monolayer. We speculate that at low pressures the surface-confined ferrocene/ferrocenium couple, does not experience large volume constraints, perhaps because ion pairing and the extent of aggregation are not significantly altered in the low pressure range. However, as pressure increases, volume effects become noticeable. Several factors may be responsible: (1) pressure-disruption of ion pairing and (2) pressure-enhancement of ferrocene aggregation. Both factors are, at least in part, a consequence of the change in the dielectric constant of water (ϵ_w) brought about by compression (ϵ_w increases by $\approx 25\%$ at 5.8 kbar[4]).

In general, due to the electrostriction effect, pressure promotes the dissociation of ion pairs. The electrostriction effect,[29,30] which can be described as the contraction of solvent molecules around a charged species, causes a net decrease in volume that is responsible for the negative volume changes observed for many dissociation reactions.[3-5,30] Also, as ϵ_w increases with compression, so will in turn the negative volume of electrostriction. Thus, in principle, we expect the dissociation below (8) to have a negative volume of reaction (ΔV°_d) and, according to expression (9), to be favored with compression.

$$FeCp_2^+ClO_4^-(SAM) \leftrightarrow FeCp_2^+(SAM) + ClO_4^-(aq) \tag{8}$$
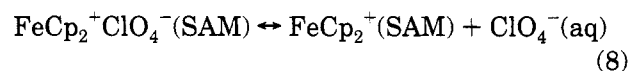
$$(\partial \Delta G^{\circ}/\partial P)_T = -RT(\partial \ln K^{\circ}_d/\partial P)_T = \Delta V^{\circ}_d \tag{9}$$

Here ΔG° denotes the standard free energy of dissociation and $K^{\circ}_{d(P)}$ the standard dissociation constant for equilibrium (8) at pressure P. If ΔV°_d is pressure independent, it follows that the pressure dependence of $K^{\circ}_{d(P)}$ can be expressed as

$$K^{\circ}_{d(P)} = K^{\circ}_{d(P=0kbar)} \exp(-\Delta V^{\circ}_d/RT)P \tag{10}$$

Since the standard redox potential for the ferrocene/ferrocenium half-reaction in equilibrium (5) and $K_{d(P)}$ are related according to (11), we reason that an increase in

(31) le Noble, W. J. *Rev Phys. Chem. Jpn.* **1980**, *50*, 207.

$$E°_{(P)(\text{FeCp}_2{}^+\text{ClO}_4{}^--(\text{SAM})/\text{FeCp}_2(\text{SAM}))} =$$

$$E°_{(P)(\text{FeCp}_2{}^+(\text{SAM})/\text{FeCp}_2(\text{SAM}))} + (RT/nF) \ln K°_{d(P)} \quad (11)$$

$K°_d$, caused by increasing pressures, will raise the redox potential. Therefore, we expect the higher pressures to partially break the association of the perchlorate and ferrocenium ions, especially those located in the assembly's outer layer, closer to the aqueous solvent (of increasingly higher ϵ_w), rendering oxidation *energetically more difficult*. As explained earlier, the driving force for dissociation, originating from electrostriction, would be provided mainly by the perchlorate ion and not the ferrocenium ion. The perchlorate ion is a rather lipophilic ion[16] itself, with a calculated hydration volume of only -1.6 mL/mol. So we believe that ion-pair disruption alone does not explain the pressure dependence of the redox potential for the surface-confined ferrocene/ferrocenium couple.

The other possible factor is that the aggregation of ferrocene might be enhanced with application of pressure, through both compression itself and a rise in the dielectric constant of water. With an increase in ϵ_w we expect the ferrocene groups to tend to hide away from the aqueous medium and aggregate even more at high pressures. Then, at the upper pressure end, as aggregation is enhanced, ion incorporation must become hindered, yet more needed for oxidation to occur. And as the aggregates are more difficult to break, part of the ferrocenes become electroinactive. Consequently, oxidation becomes *sterically disfavored*. At the same time, pressure-promoted aggregation of the redox sites should also expose the redox sites to decreasingly polar vicinities and raise the redox potential as we observe, rendering oxidation *energetically disfavored* also. Analogously, Rowe and Creager[16a] found that by systematically varying the length of spacer alkyl chains surrounding pendant ferrocene groups they could expose the ferrocene centers to decreasingly polar environments and cause an increase in redox potential. However, the changes in redox potential that they obtained appeared to be thermodynamic in nature and did not show an asymmetry like the one displayed in Figure 4.

Incidentally, an asymmetry similar to that in Figure 4 is seen for all samples at individual pressures when ΔE_{pa} or ΔE_{pc} is plotted against scan rates (v) (Figure 5). Here again one can infer that oxidation and reduction kinetics are affected by overpotential in different ways. This asymmetry suggests again that oxidation and reduction steps encounter differing kinetic limitations, perhaps because the reaction follows a square-scheme type of path.

Chronoamperometric Studies. Since our data on peak separation vs scan rate did not allow an accurate Laviron analysis[32] (an accurate Laviron analysis requires peak separations above 200 mV, which in our systems were encountered at scan rates and pressures so high that good definition of cyclic voltammetric peaks was prevented), we have conducted chronoamperometric measurements to estimate the change in rate of electron transfer as a function of pressure. Chronoamperometry determinations[33,34] render rate constants provided that single exponential faradaic current decays are obtained. The latter are expected when the monolayer possesses a homogeneous population of redox centers. According to the expression below (12), rate constants (k) can be extracted from the linear slope of semilogarithmic plots.
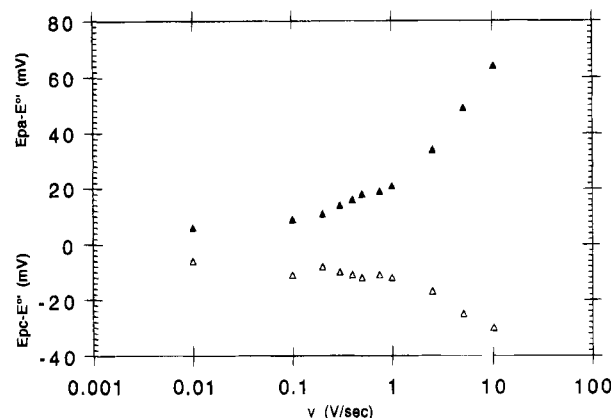

Figure 5. Cyclic voltammetric peak potential at any scan rate minus redox potential ($E°'$) at 10 mV/s vs scan rate. Key: solid triangles, anodic (oxidation) peak; hollow triangles, cathodic (reduction) peak. SAM sample 3 in 1 M NaClO₄; $P = 0$ kbar.

$$\ln i_F = \ln kQ - kt \quad (12)$$

where i_F denotes the faradaic current that evolves during the potential step, Q is the charged passed during the redox process, and k is the rate constant at the overpotential employed.

In general, due to the rather heterogeneous nature of our monolayer assemblies, we did not observe single exponential decays. Nevertheless, preliminary results show that, under compression, and by varying the overpotential window, the anodic (oxidation) current decays show regions of linearity which we use to estimate the pressure-induced change in the rate of electron transfer for the oxidation step and, thus, volumes of activation ($\Delta V^{\ddagger}$s) for oxidation. Semilogarithmic plots for the anodic currents corresponding to sample 3 can be found in Figure 6. Here we see that, in qualitative agreement with our CV data, (1) the total charge evolved during the potential step diminishes with compression and (2) the overall rate of charge evolution decreases with compression also. At an overpotential of 80 mV, nearly linear regions are observed at all pressures. We define two dominant regions within the semilogarithmic graphs. One at earlier times, below 1–2 ms, which we call k_f. This type of CA response, indicative of the existence of an initial fast process, has been observed for other monolayer systems,[33] but in our case the origin of such process is not well-understood at present. Above 1–2 ms, we define a dominant rate constant, k_s, which corresponds to a slower process. Table 4 shows the k_s values that we have determined from CA semilogarithmic plots. Due to kinetic heterogeneity, the measured k_s values represent an *average* rate constant[17] for a distribution of ferrocene sites corresponding to only a fraction of the total electroactive population. This average rate constant allows us to estimate $\Delta V^{\ddagger}$s for the purpose of corroborating conclusions drawn from our CV data. From (4) we calculate volumes of activation for the slower oxidation process, $\Delta V^{\ddagger} = -RT (\ln k_s{}^{P2} - \ln k_s{}^{P1})/(P_2 - P_1)$, and present them in Table 5. The positive volumes of activation that we find are indexes of the volume change associated with the oxidation transition step and confirm our expectation of a volume expansion that either precedes, accompanies, or follows the oxidation process. Analysis of the cathodic process shows that the reduction currents follow nonlinear decays that are similar in magnitude to those observed for the oxidation currents at ambient pressure; however, they are pressure independent (the effect of overpotential was not investigated). Therefore, it appears that, under compression, the reduction process is faster than the oxidation and volume indepen-

(32) Laviron, E, *J. Electroanal. Chem.* **1979**, *101*, 19.
(33) Finklea, H. O.; Hanshew, D. D. *J. Am. Chem. Soc.* **1992**, *114*, 9.
(34) Forster, R. J.; Faulkner, L. R., *J. Am. Chem. Soc.* **1994**, *116*, 5444; *J. Am. Chem. Soc.* **1994**, *116*, 5453.
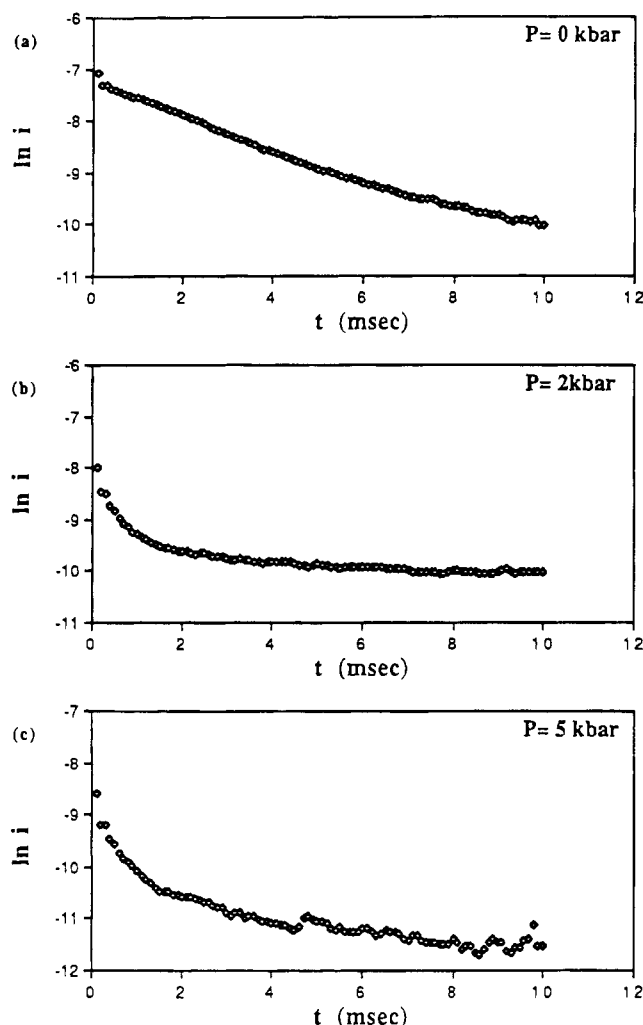
Figure 6. Semilogarithmic plots for the chronoamperometric anodic current of ferrocene/ferrocenium in SAM, 1 M $NaClO_4$, at various pressures (Sample 3). Overpotential η = 80 mV. According to our impedance measurements R_u (uncompensated resistance) = 40 Ω, and C_d = 0.045 μF, so double layer charging is complete during the first 10 μs of the experiment.

Table 4. Average Rate Constant, k_s (ms^{-1}) vs P at Various Overpotentials $(\eta)^d$ (Sample 3)

P (kbar)	η = 0 mV	η = 80 mV	η = 130 mV	η = 180 mV
0		0.29	a	a
1	0.05^c	0.10	0.18	0.23
2	0.02^c	0.05	0.09	0.13
3		b	0.09	0.10
4		b	b	0.10
5		0.10	0.10	0.10
release		0.28	a	a

^{a} No linear-decay regions observed. ^{b} Not measured at this η. ^{c} $k°$, standard heterogeneous rate constant, calculated from the intercept of the Tafel plot. ^{d} Potential limits were varied to keep each η constant at all pressures.

Table 5. Estimates of Volumes of Activation for the Oxidation, $\Delta v^\ddagger$ (mL/mol), Calculated from k_s at P and η at Which Enough Data Are Available (Sample 3)

P (kbar)	η = 0 mV	η = 80 mV	η =130 mV	η = 180 mV
0		26		
1	19	17	17	14
2			0	6
3				0

dent. This would imply that no sterical hindrance exists when ferrocenium is converted to a neutral ferrocene in the monolayer and would reinforce the idea of an asym-

Table 6. Capacitance Measurements at High Pressure for Two SAM Samples in 1 M $NaClO_4$ (E_{dc} = 0 mV; E_{ac} = ±2 mV; f = 1–10 kHz)

	C_d (μF/cm^2)			C_d (μF/cm^2)	
P (kbar)	sample 3	sample 4	P (kbar)	sample 3	sample 4
0	1.46	1.56	4	1.46	1.53
1	1.46	1.56	5	1.46	1.53
2	1.48	1.56	release	1.45	1.53
3	1.46	1.53			

metry of kinetic origin inferred from the data presented in Figure 4.

Tafel plots[35] constructed by linearly fitting the rate constants shown in Table 4 at pressures 1 and 2 kbar (correlation coefficients 0.943 and 0.983, respectively) provide transfer coefficient values (α) of 0.78 at 1 kbar and 0.75 at 2 kbar. This value (α > 0.5) is consistent with our cyclicvoltammetric and chronoamperometric data pointing again at the asymmetric nature of the redox process. We attribute the asymmetry to the need for ion complexation and/or a structural rearrangement occurring on oxidation.

Interfacial Capacitance Measurements. To determine whether a pressure-induced structural transition could be responsible for the high-pressure behavior of our monolayer systems, we also performed capacitance measurements. With interfacial capacitance values we can assess the degree of compactness of the assembly and the average thickness of the monolayer. The interfacial capacitance is equivalent to a parallel-plate capacitor defined, in our system, by the excess charge on the gold electrode surface and the solution ionic countercharge on the plane next to the monolayer. The high concentration of electrolyte that we employ (1 M) allows us to use the Helmholtz[35] model of the double layer. In accordance with this model, the double layer capacitance (C_d) is inversely proportional to the average distance between the two charge planes (d) and directly proportional to the dielectric constant of the medium (the alkyl chains and ferrocene groups) and the permitivity of free space (ϵ_0),

$$C_d = \epsilon\epsilon_0/d \tag{12}$$

Our capacitance values, derived from Impedance or Nyquist plots[35] obtained from impedance measurements conducted in either 1 M $NaClO_4$ or $NaNO_3$, at a reducing dc potential, ranged between 1.4 and 2.1 μF/cm^2. These values are similar to those previously reported[7] for alkyl chain monolayers. Such low capacitance values are indicators of a true nonpolar medium impermeable to water, at least in the reduced state of the monolayer. High-pressure capacitance measurements were done on electrode samples 3 and 4. The results are listed in Table 6 and show that no change in double layer capacitance occurs for the reduced monolayer under pressure. Moreover, assuming the dielectric constant of the organic medium to be that of polymethylene, that is, 2.26, which, according to the Clausius–Mossotti expression,[4] varies negligibly with pressure, the average monolayer thickness value that we obtain is ≈13 Å at all pressures. This value suggests that at all pressures the chains in the reduced monolayer are in a disordered arrangement composed of bent and extended chains (the monolayer thickness expected for an assembly of all-extended chains at 90° from the electrode surface is 26 Å and at 30° from the surface is 23 Å). On the basis of these determinations, we find no evidence for a pressure-induced structural transition of

(35) Bard, A. J.; Faulkner, L. R. *Electrochemical Methods—Fundamentals and Applications*; Wiley & Sons, Inc: New York, 1980.

the ferrocene monolayer (in the reduced state). That is, significant rearrangements of the monolayer such as pressure-enhanced alignment of the chains (through stretching), further contraction of the layer (through folding), or water and/or ion inclusion are unlikely. Nevertheless, we believe a lateral transformation, such as aggregate formation or aggregate disruption, would still be possible. Such a transformation could interfere greatly with the oxidation of ferrocene if desaggregation is required to form an ion pair. These aggregational changes may be equivalent to those observed[36] when two-dimensional pressures are applied to Langmuir–Blodgett-films. Surface pressures can enhance the aggregation of the molecules in the Langmuir–Blodgett-monolayers to varying degrees, depending on the electrostatic charge of the head group and can give rise to a range of 2D compressibilities. For instance, the neutral ones,[36] like those containing both a positive and a negative functionality on the same end group (zwitterionic) are more compressible than those with a net charge. In an analogous manner, our neutral ferrocene groups would permit further aggregation of the head groups and compress more than the charged ferrocenium ions. As far as the lack of variability of C_d with pressure is concerned, we should comment that compensation effects, such as an increase in dielectric constant, due to water penetration, and an increase in d, owing to extension of the alkyl chains, are also possible. However, we think it is very unlikely that such an effect will take place while giving rise at the same time to the striking constancy of C_d values displayed in Table 6.

Conclusions

By means of high pressures and electrochemical techniques we have explored the thermodynamics and kinetics of charge transfer in ferrocene-terminated monolayers placed on electrode surfaces. The pure ferrocene monolayer assemblies that we have prepared appear to be rather disordered and show electrochemical responses indicative of attractive interactions among redox centers (aggregation) and heterogeneities within the assemblies. We found that the oxidation of surface-bound neutral ferrocene to ferrocenium is disfavored with compression. We attribute this effect to the steric characteristics of the oxidation step, which involves a volume expansion relative to that of ferrocene in solution, probably related to a structural transformation of the monolayer and a need for counterion complexation. We also found that different monolayer
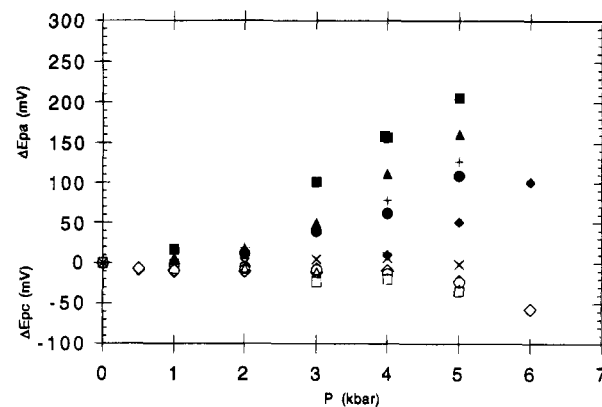
(36) Song, Q.; Bohn, P. W. Pittsburgh Conference on Analytical Chemistry and Applied Spectroscopy, Chicago, February 1994, Abstract 135P.

Figure 7. Results for SAM sample 5, immersed in 1 M $NaNO_3$, are added to those in Figure 4 for a comparison [+, anodic peak (ΔE_{pa}); x, cathodic peak (ΔE_{pc})]. Scan rate, 100 mV/s.

samples impose different volume constraints on the oxidation process. Therefore, we conclude that each and every different sample can possess differing degrees of ordering and redox site interactions and, thus, can place the ferrocene groups in different spatial arrangements and expose them to varying degrees of polarity and solvent and ion accessibility. We have also included data for the ferrocene/ferrocenium couple dissolved in aqueous 1 M $NaClO_4$ and in SAMs immersed in 1 M $NaNO_3$ ($v = 30$ mL/mol)[29] instead of 1 M $NaClO_4$ ($v = 44.6$ mL/mol),[29] to show that the observed pressure behavior is related to the surface-confinement of ferrocene rather than solely to the nature of the counterion (Figure 7).

In addition, we have shown that high-pressure techniques can be very well utilized in the investigation of interfacial systems and phenomena. Here we demonstrate that high-pressure techniques can provide information on the volume effects within monolayer assemblies that was not available before. Optimal utilization of the high-pressure technique should be attained by studying monolayer systems of better defined and controlled architecture.